

This article was downloaded by: [Siauliu University Library]

On: 17 February 2013, At: 07:01

Publisher: Taylor & Francis

Informa Ltd Registered in England and Wales Registered Number: 1072954 Registered office: Mortimer House, 37-41 Mortimer Street, London W1T 3JH, UK



Advanced Composite Materials

Publication details, including instructions for authors and subscription information:

<http://www.tandfonline.com/loi/tacm20>

Impact damage and CAI strength of MR50K/PETI5 carbon/tough-polyimide composite at room and high temperatures

Hisaya Katoh , Toshiyuki Shimokawa , Akira Ueda , Daisuke Kobayashi & Yasumasa Hamaguchi

Version of record first published: 02 Apr 2012.

To cite this article: Hisaya Katoh , Toshiyuki Shimokawa , Akira Ueda , Daisuke Kobayashi & Yasumasa Hamaguchi (2005): Impact damage and CAI strength of MR50K/PETI5 carbon/tough-polyimide composite at room and high temperatures, *Advanced Composite Materials*, 14:2, 211-228

To link to this article: <http://dx.doi.org/10.1163/1568551053970654>

PLEASE SCROLL DOWN FOR ARTICLE

Full terms and conditions of use: <http://www.tandfonline.com/page/terms-and-conditions>

This article may be used for research, teaching, and private study purposes. Any substantial or systematic reproduction, redistribution, reselling, loan, sub-licensing, systematic supply, or distribution in any form to anyone is expressly forbidden.

The publisher does not give any warranty express or implied or make any representation that the contents will be complete or accurate or up to date. The accuracy of any instructions, formulae, and drug doses should be independently verified with primary sources. The publisher shall not be liable for any loss, actions, claims, proceedings, demand, or costs or damages whatsoever or howsoever caused arising directly or indirectly in connection with or arising out of the use of this material.

Impact damage and CAI strength of MR50K/PETI5 carbon/tough-polyimide composite at room and high temperatures

HISAYA KATOH^{1,*}, TOSHIYUKI SHIMOKAWA², AKIRA UEDA³,
DAISUKE KOBAYASHI⁴ and YASUMASA HAMAGUCHI¹

¹Advanced Composites Evaluation Technology Center (ACE-TeC), Japan Aerospace Exploration Agency (JAXA), 6-13-1 Ohsawa, Mitaka, Tokyo 191-0015, Japan

²Department of Aerospace Engineering, Tokyo Metropolitan Institute of Technology (TMIT), 6-6 Asahigaoka, Hino, Tokyo 191-0065, Japan

³Toyota Motor Corp., 1, Toyota-Cho, Toyota, Aichi 471-0826, Japan

⁴Komatsu Forklift Co. Ltd., 110 Yokokura-Shinden, Oyama, Tochigi 323-0819, Japan

Received 10 September 2004; accepted 18 November 2004

Abstract—This study determined the compression-after-impact (CAI) behavior and strength of a carbon/tough-polyimide composite material, MR50K/PETI5, whose PETI5 resin has been specially developed for the next generation supersonic transport (SST) at NASA. First, an impact test imposed impact damage on CAI specimens at room temperature, and the load and absorbed energy were measured; in addition, the damage was examined with an ultrasonic C-scanner and a 3D ultrasonic inspection system. Second, CAI strength and failure strain were measured at room temperature and at 180°C. Third, the damage induced by the CAI test was examined with an optical microscope. Test results were compared with those of T800H/PMR-15 carbon/polyimide composite, where PMR-15 is a typical brittle resin, and the characteristic CAI behavior and strength of a carbon fiber/highly-tough resin composite were determined.

Keywords: CFRP; MR50K/PETI5; T800H/PMR-15; CAI strength; CAI failure strain; impact damage; 3D damage image; compressive failure mode.

1. INTRODUCTION

Carbon fiber/polymer matrix composites (CFRP) are widely used as indispensable aircraft structural materials. However, CFRP should be used only for structures that

*To whom correspondence should be addressed. E-mail: katoh.hisaya@jaxa.jp

are not subjected to heating during flight, because of the poor thermal resistance of the epoxy resins generally used. On the other hand, since the out-of-plane strength of laminated epoxy CFRPs is usually low, compressive strength and CAI strength are frequently used in structural design criteria. In this respect tough resins are desirable and attractive for practical use. Moreover, a tough-resin CFRP is scientifically interesting, because such a resin is expected to show improved mechanical properties and different behavior from that seen in common epoxy CFRPs.

Recently, new high heat-resistant and tough polyimide resins have been developed in Japan and the USA in order to expand CFRP applications in the high temperature regime. Among them, PETI5 polyimide resin was developed by NASA as a resin having both high heat-resistance and outstanding toughness for use in the structures of a commercial high-speed civil transport (HSCT).

Some basic mechanical properties of CFRPs with PETI5 resin have already been investigated. Hou *et al.* [1] investigated the manufacturing process of a CFRP with PETI5 and the basic mechanical properties of 0 degree lamina and the open-hole compression (OHC) strength of a laminated material. Walker [2] experimentally investigated the compressive strength of IM7/PETI5 at three temperatures, calculated the residual interlaminar shear stresses using three dimensional FEM, and reported that their effect on the compressive strength was small. Moreover, Hergenrother [3] has introduced experimental data on the OHC strength, CAI strength, CAI elastic modulus, tensile and compressive strength of 0 degree lamina and a quasi-isotropic laminate of IM7/PETI5 CFRP from unpublished papers, reviewing structural composite and other materials for the next-generation supersonic transport. However, with respect to the CAI strength and modulus in Ref. [3], there is no description about the impact load level or details of testing conditions. Therefore, it can be considered that there is still no available report of the impact behavior and CAI strength of PETI5 CFRPs.

The objective of this study is to investigate experimentally the impact damage and CAI strength of a MR50K/PETI5 composite material with a stacking sequence $[-45/0/45/90]_{4S}$. The contents of this report are as follows. (1) CAI specimens of MR50K/PETI5 were subjected to impact damage at room temperature. Load and absorbed energy were measured during impact loading. (2) The impacted specimens were examined with an ultrasonic C-scanner and a 3D ultrasonic inspection system. (3) The CAI strength at room and high temperatures was investigated. (4) The cross-sectional area cut from the CAI failure specimens was examined to study the failure mode. (5) Some test results are compared with those of T800H/PMR-15, a typical carbon/brittle-polyimide composite material. (6) Typical and fundamental post-impact compressive-failure behaviors of a CFRP using a highly tough resin are presented.

2. MATERIALS, SPECIMEN AND TESTING PROCEDURE

2.1. Material and specimen

The material selected for this study was MR50K/PETI5 carbon fiber/polyimide resin composite material. MR50K is a medium-elastic carbon fiber without any sizing treatment, produced by Mitsubishi Rayon Co. PETI5 is a polyimide resin developed by NASA for HSCT structures and produced by Cytec Co. MR50K fiber and PETI5 resin are considered to be a good match by composite engineers in Japan. On the other hand, a typically brittle and high heat-resistant T800H/PMR-15 carbon fiber/polyimide resin composite material was chosen for comparison of CAI properties. In a joint research program of the National Aerospace Laboratory (NAL) and the National Space Development Agency in Japan (NASDA), large body of design data were acquired on T800H/PMR-15, a candidate structural material for the small unmanned space shuttle HOPE-X.

The authors have previously reported the CAI characteristics of T800H/PMR-15 [4]; however, the material used in the study was considered more brittle than normal T800H/PMR-15 materials. This paper uses only the test results for impact response and delamination produced in the T800H/PMR-15 laminate presented in Ref. [4] for comparison. The CAI strength of a normal T800H/PMR-15 obtained by Fuji Heavy Industries (FHI) and NASDA [5] is used for comparison, as described later.

The stacking sequence of the material tested is quasi-isotropic 32-ply $[-45/0/45/90]_{4S}$, which is generally used in CAI and compression tests. Figures 1 and 2 show the specimen configuration and impact test fixture for CAI tests, respectively. The sizes and shapes of the specimen and fixture are based on SACMA SRM2R-94.

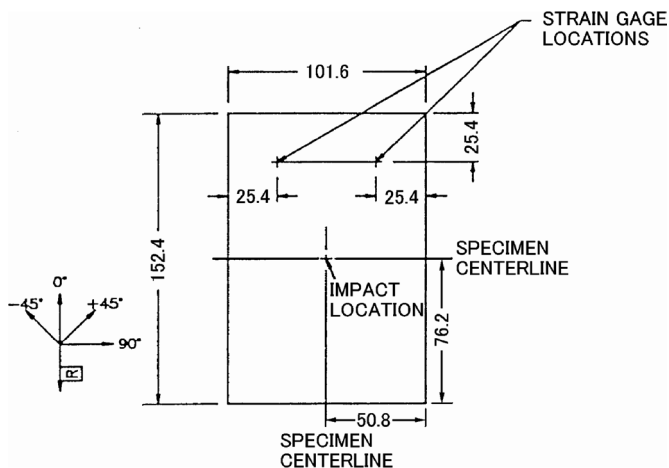


Figure 1. CAI specimen configuration.

2.2. Testing procedure

The impact test procedure is as follows: A specimen is fixed in the support fixture with the rubber head toggle clamp as illustrated in Fig. 2, the impactor load is applied to the center of the specimen by an INSTRON 9250 impact testing machine. The impactor weight is 5.07 kg with a semi-spherical head of radius 15.9 mm. When the specimen was impact-loaded, the impact load vs. time of response was measured using a load cell installed inside of the impactor as well as the impactor velocity just before striking the specimen. The strain energy absorbed by the specimen was automatically calculated and recorded with a function program built in the impact machine.

The surface impact damage was examined with an optical microscope, and then an ultrasonic C-scanner was used to examine the delamination inside of the specimen from both specimen surfaces. Additionally, the three-dimensional damage inside an impacted specimen was recorded with a Toshiba three-dimensional (3D) ultrasonic inspection system with 256 ultrasonic sensors.

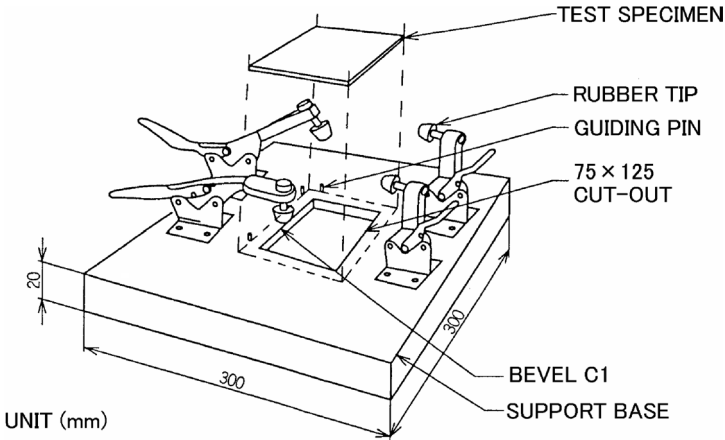


Figure 2. Impact test fixture.

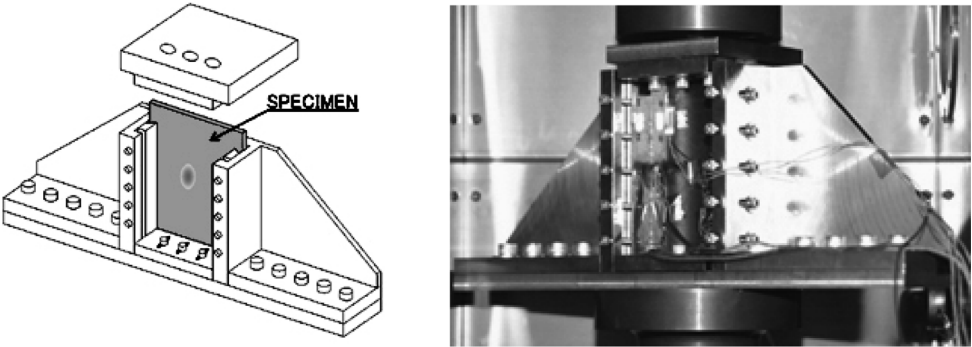


Figure 3. Compression-after-impact test fixture and test setup.

After ultrasonic inspections, the impacted specimen was equipped with four strain gauges as shown in Fig. 1, two on each surface and secured in the compression-after-impact (CAI) test fixture as shown in Fig. 3. Compression tests were conducted at a displacement speed of 1.0 mm/min and the load–displacement relationship was measured.

The compression tests were carried out at room temperature and 180°C. The tests used an Instron 1128 type mechanical material-testing machine at room temperature, and at 180°C used an Instron 8500 type digitally controlled servo-hydraulic material-testing machine with an environmental chamber. This compression test fixture and testing method were based on SACMA SRM2R-94.

After the compression test, the specimen was machined along the loading axis passing through the impacted point, and the cut section was polished for examination with an optical microscope. The failure mode is discussed based on the damage state generated by impact and compression loads.

3. TEST RESULTS AND DISCUSSION

3.1. Load and absorbed energy response for impact load

Four levels of impact energy, 2.22, 4.45, 6.67, and 8.90 J/mm normalized by nominal specimen thickness, were applied to MR50K/PETI5 specimens. Meanwhile, three levels of impact energy, 2.22, 4.45, and 6.67 J/mm were applied to T800H/PMR-15 specimens. Figure 4 shows the time response curves of the load and absorbed energy during impact tests of MR50K/PETI5 specimens. Figure 5 presents those of a T800H/PMR-15 specimen. For the MR50K/PETI5 specimens, the impact load as a function of time showed a trapezoidal shape at 4.45 J/mm or higher, though it was a parabolic shape at 2.22 J/mm. For T800H/PMR-15 specimens, the shape is parabolic with small ripples superimposed. Comparing the load response curves of the two kinds of CFRPs, the trapezoidal shape produced by the MR50K/PETI5 specimens is considered to be due to the deformation of a highly tough resin. Meanwhile the general tendency of absorbed energy response curves in Figs 4 and 5 at the same impact energy is not so different. This is because the numerical formula of absorbed energy includes no direct load-response term but the terms of single and double integrals and the square of a single integral for the load response.

Figure 6 shows the relationship between the maximum load and impact energy. In the case of MR50K/PETI5, the maximum load generated at an impact energy of 2.22 J/mm is 8.1 kN, and that from 4.45 to 8.90 J/mm is almost constant at 10 kN. However, the holding time near the maximum load grows longer as impact energy increases, as shown in Fig. 4. In the case of T800H/PMR-15, the maximum load increases rapidly with impact energy. The deformation of a highly tough resin can absorb a lot of impact energy; meanwhile, a brittle matrix cannot absorb much impact energy due to its small acceptable deformation. The absorbed energy

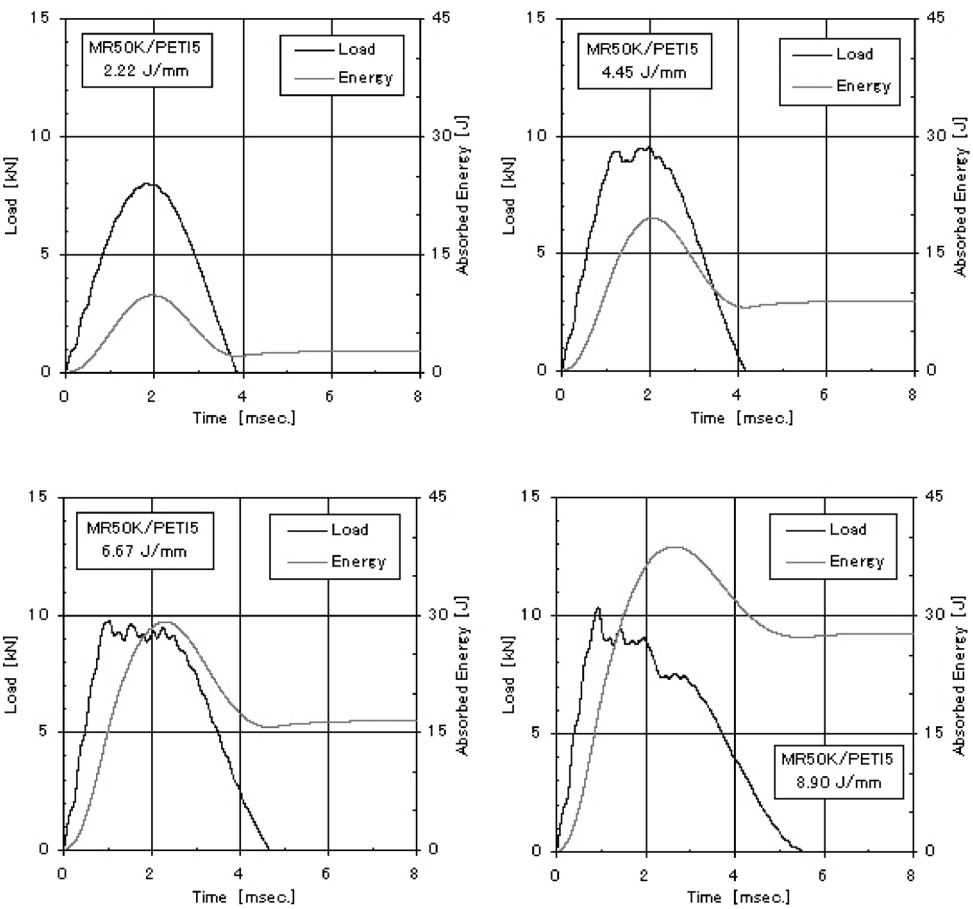


Figure 4. Load and absorbed energy during an impact test for MR50K/PETI.

retained after an impact test is considered to have been consumed in producing damage inside the specimen. This study designates this energy as the ‘residual absorbed energy’. This is defined by the absorbed energy when the load response returns to zero. Figure 7 presents the relationship between residual absorbed energy and impact energy. Residual absorbed energy increases approximately in proportion to impact energy, and their relationship is identical for both MR50K/PETI5 and T800H/PMR-15. It is worth noting that the residual absorbed energy is not changed by the toughness of the resin.

3.2. Impact damage and delamination area

3.2.1. Surface observation. Surface inspection of a MR50K/PETI5 specimen after impact tests found an impact mark with a deep dent. Furthermore, when impact energy was high, cracks along the 45° fiber orientation were observed on the surface around the impact mark. The area and dent depth of the impact marks

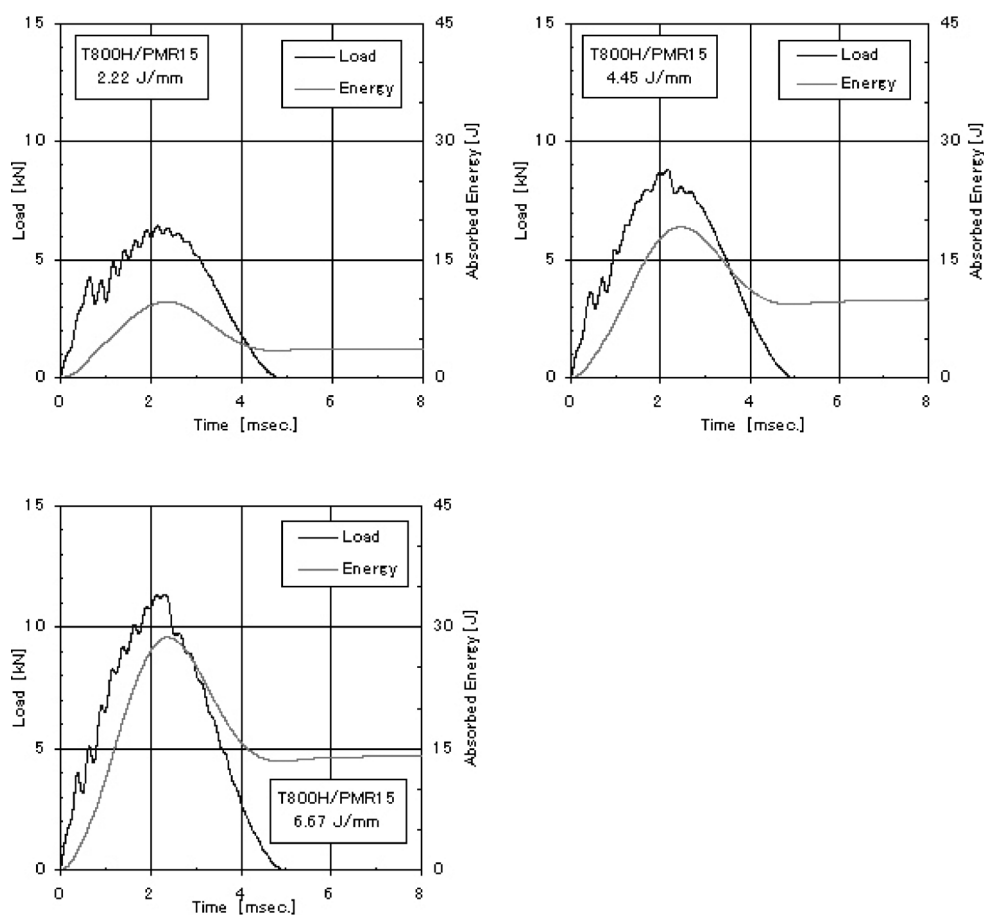


Figure 5. Load and absorbed energy during an impact test for T800H/PMR-15.

of MR50K/PETI5 specimens were larger than those that appeared in T800H/PMR-15 specimens. However, the appearance on the surface opposite the impact marks was not much different in both materials. Since the residual absorbed energy at the same impact energy was identical for both materials, as described before, these facts mean that more energy was consumed in producing an impact mark and cracking in MR50K/PETI5 specimens rather than in T800H/PMR-15 specimens.

3.2.2. Observation of delamination by an ultrasonic C-scanner and a 3D inspection system. An ultrasonic C-scanner was used to investigate the impact damage, which consisted mainly of delamination accompanying small cracks in the laminae; however, only the delamination is discussed below. Figure 8 shows the ultrasonic B- and C-scope inspection results for MR50K/PETI5 specimens subjected to impact energies from 2.22 to 8.90 J/mm. Figure 9 presents corresponding results for T800H/PMR-15 specimens impacted at energy levels from 2.22 to 6.67 J/mm.

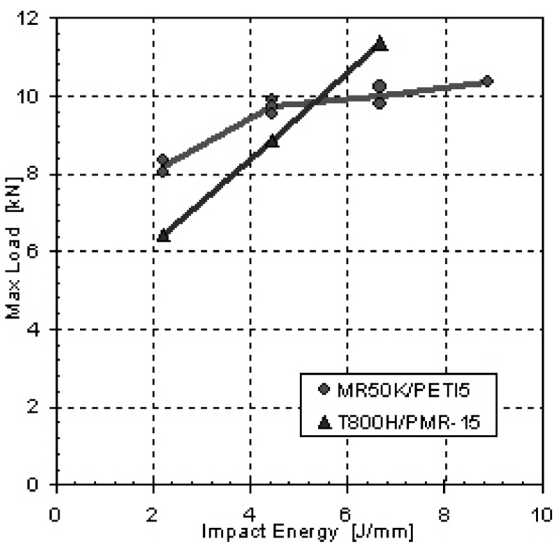


Figure 6. Maximum load vs. impact energy.

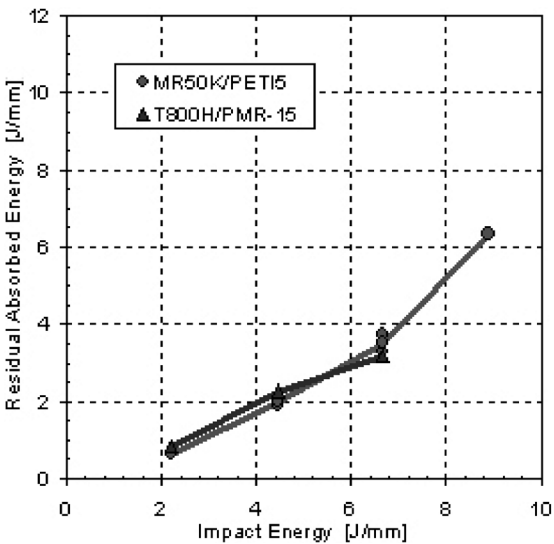


Figure 7. Residual absorbed energy vs. impact energy.

Furthermore, Fig. 10 shows a three dimensional image of the impact damage inside a MR50K/PETI5 specimen after the impact test at 4.45 J/mm. This picture was taken by a 3D ultrasonic inspection system. A rather small damage area expands between laminae and the helical pattern of damage progression is confirmed. The top surface is the impacted portion, and considered to have suffered mainly resin damage. When the delamination is viewed from the top surface looking towards the bottom surface, this picture shows that the delamination

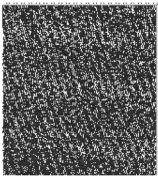
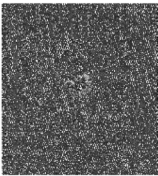






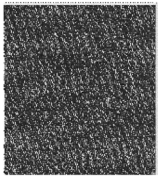
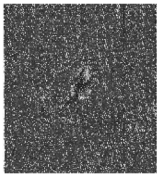
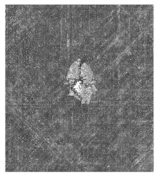

Impact Energy	2.22 J/mm	4.45 J/mm	6.67 J/mm	8.90 J/mm
C-Scope (Upper Surface)				
B-Scope				
C-Scope (Lower Surface)				
Details	Area 0 mm ² Width 0 mm	Area 189 mm ² Width 19.9 mm	Area 340 mm ² Width 21.7 mm	Area 357 mm ² Width 27.2 mm

Figure 8. Delamination of MR50K/PETI5 observed by ultrasonic C-scanner at four impact energy levels.

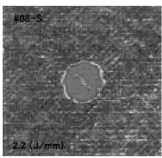
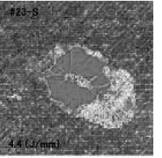
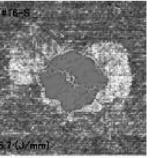



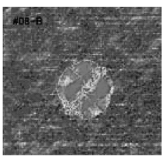
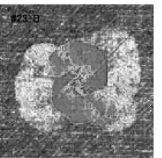
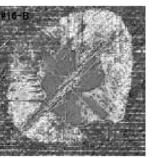
Impact Energy	2.22 J/mm	4.45 J/mm	6.67 J/mm
C-Scope (Upper Surface)			
B-Scope			
C-Scope (Lower Surface)			
Details	Area 906 mm ² Width 34.7 mm	Area 4376 mm ² Width 82.2 mm	Area 5381 mm ² Width 82.0 mm

Figure 9. Delamination of T800H/PMR-15 observed by ultrasonic C-scanner at three impact energy levels.

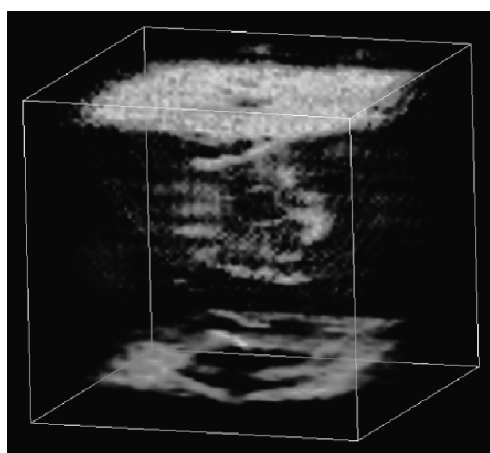


Figure 10. A three-dimensional view of the impact damage in MR50K/PETI5 from an impact energy 4.45 J/mm, obtained with a 3D ultrasonic inspection system.

progressed helically clockwise from the top to the center of the sample and with a counterclockwise turn from the center to the bottom. This phenomenon is considered to show that when the delamination progresses in the thickness direction it extends to the next lamina with a smaller angle. This study is the first to show a complete image of the progress of CAI damage inside of a laminated composite, obtained with a 3D ultrasonic inspection system.

The C-scope results in Fig. 8 show that the delamination area of MR50K/PETI5 specimens is very small in comparison with that of T800H/PMR-15 specimens at the same impact energy in Fig. 9. The B-scope results in Fig. 8 and the 3D image in Fig. 10 indicate that the distribution of the delamination in the thickness direction in MR50K/PETI5 specimens forms a cylindrical shape with a small diameter, or a drum shape having a swollen center, instead of a conical shape (in which the cross-sectional area enlarges towards the back surface) as shown in T800H/PMR-15 specimens in Fig. 9. Moreover, this picture indicates that the delamination area defined below is approximately equal to the front surface damage area.

In the following arguments, the delamination area is defined as the total area projected by every delamination area inside the specimen onto the specimen surface. The maximum delamination width is defined by the maximum lateral length, i.e. perpendicular to the load axis, of the delamination area.

Figure 11 presents the relationship between delamination area and impact energy. The delamination area increases linearly with increasing impact energy. The delamination area of a MR50K/PETI5 specimen impacted at 4.45 J/mm is only 4.7% of that in a T800H/PMR-15 specimen, and it is only 5.6% at 6.67 J/mm. The large difference in the delamination areas is thought to be caused by the difference in the interlaminar fracture toughness of the materials. Since the interlaminar fracture toughness is strongly dependent on the resin toughness, it is considered that the

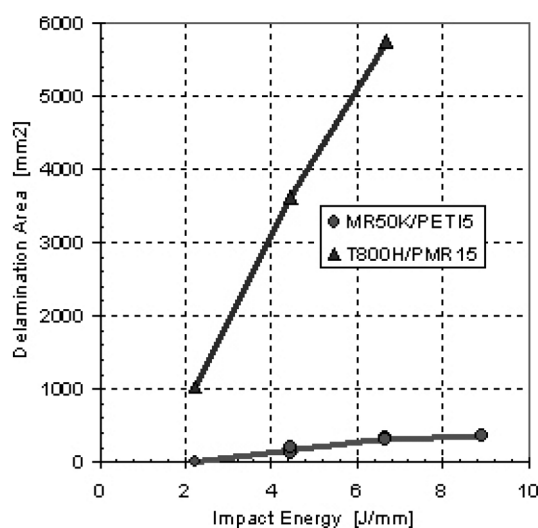


Figure 11. Delamination area vs. impact energy.

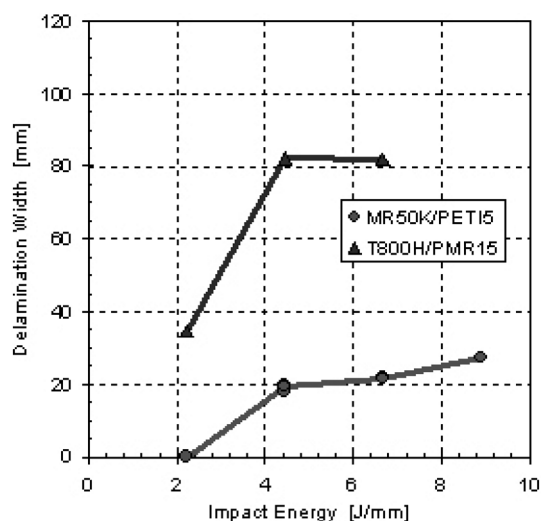


Figure 12. Delamination width vs. impact energy.

impact energy for brittle PMR-15 resin was consumed by the delamination, so that large surface-layer damage was not generated. In contrast, since the fracture toughness of PETI5 resin is remarkably high in comparison with PMR-15 resin, much of the impact energy is not absorbed by the delamination, but is consumed in generating the surface dent, surface layer cracks, or an impact mark.

Figure 12 presents the relationship between delamination width and impact energy. In the T800H/PMR-15 specimen the delamination width seems to saturate at an impact energy of 6.67 J/mm. This phenomenon is explained by the fact that

the delamination width was so great that it extended to the end of the support fixture window. Except for this case, the delamination width increases with increasing impact energy.

3.3. Compression-after-impact test results

After MR50K/PETI5 specimens were impacted, compression tests were conducted at room temperature and 180°C. Figure 13 shows CAI strength vs. impact energy relationships. In addition, the compression strength of an unnotched and non-impacted MR50K/PETI5 coupon specimen measured by the authors is plotted at an impact energy of zero J/mm. This specimen will hereafter be called ‘a non-impacted coupon specimen’. The CAI strength of T800H/PMR-15 specimens at room temperature plotted in Fig. 13 was obtained from FHI and NASDA [5], because the T800H/PMR-15 specimens that were tested in this study seemed to be too brittle, as described before. Our data were not considered appropriate for comparisons with the MR50K/PETI5 specimens.

For MR50K/PETI5 specimens, the CAI strength shows an approximately linear decrease with increasing impact energy both at room temperature and 180°C. This tendency also holds for the static strength of a non-impacted specimen at room temperature. The CAI strength of MR50K/PETI5 specimens at room temperature is 1.8 times that of T800H/PMR-15 specimens at 2.22 J/mm, two times at 4.47 J/mm, and 2.2 times at 6.67 J/mm where a MR50K/PETI5 specimen was severely damaged. On the other hand, the CAI strength of MR50K/PETI5 specimens at 180°C is about 70–80% of that at room temperature. However, even these values are far higher than those of T800H/PMR-15 specimens at room temperature.

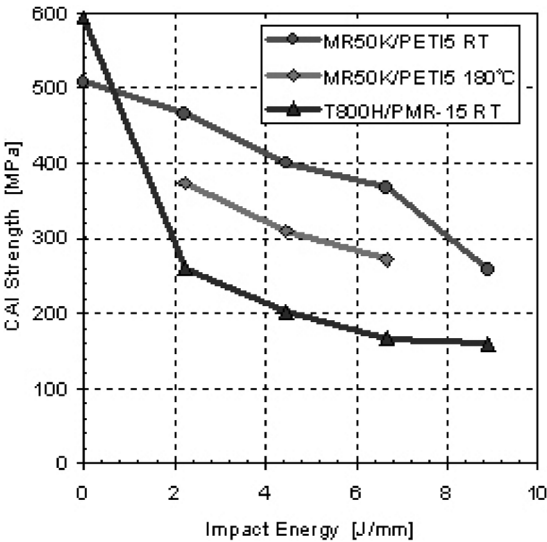


Figure 13. CAI strength vs. impact energy.

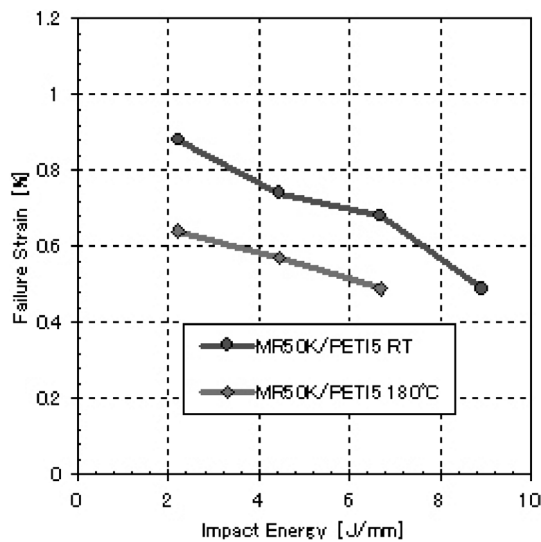


Figure 14. Failure strain vs. impact energy.

Conversely, the static compressive strength of a non-damaged MR50K/PETI5 specimen at room temperature is 17% lower than that of a T800H/PMR-15 specimen. That is, we found that though this highly tough resin has a relatively low compressive strength at room temperature, the damage generated by an impact is small, resulting in only small reduction of the CAI strength.

Figure 14 shows the relationship between failure strain and impact energy for MR50K/PETI5 at room temperature and 180°C. Similar to the CAI strength reduction in Fig. 13, the failure strain decreases linearly with the impact energy. The failure strain at 180°C decreased to about 70–80% of that at room temperature. However, since the failure strain is about 4800 $\mu\text{m}/\text{m}$ even at 8.9 J/mm and room temperature, this means that PETI5 resin has a very high impact resistance.

3.4. Delamination observed on cross-section cut after CAI tests

After the compression tests, specimens were cut through the impact point along the compression load axis. The cross-section of the MR50K/PETI5 specimen was examined with an optical microscope in order to investigate the details of the delamination and the compressive failure mode. Figures 15 and 16 show the cross-sections of the specimens after CAI testing at room temperature and 180°C, respectively. In these figures, the triangular pointers indicate the impacted locations and the lower horizontal lines show the delamination length determined by ultrasonic C-scan observation after the impact tests and before the compression tests. The compression test at room temperature for the specimen impacted with 2.22 J/mm showed that the impacted location did not become a starting point for compressive failure, though this was an exceptional case. At other impact energies, the impacted location coincided with the starting point of compressive failure.

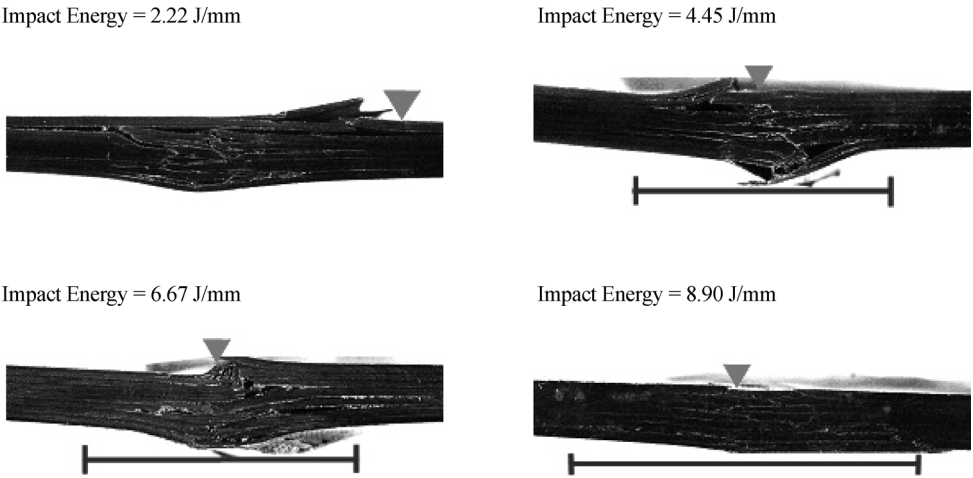


Figure 15. Impact damage and compressive failure observed on the cut section of the specimen after CAI tests at room temperature.

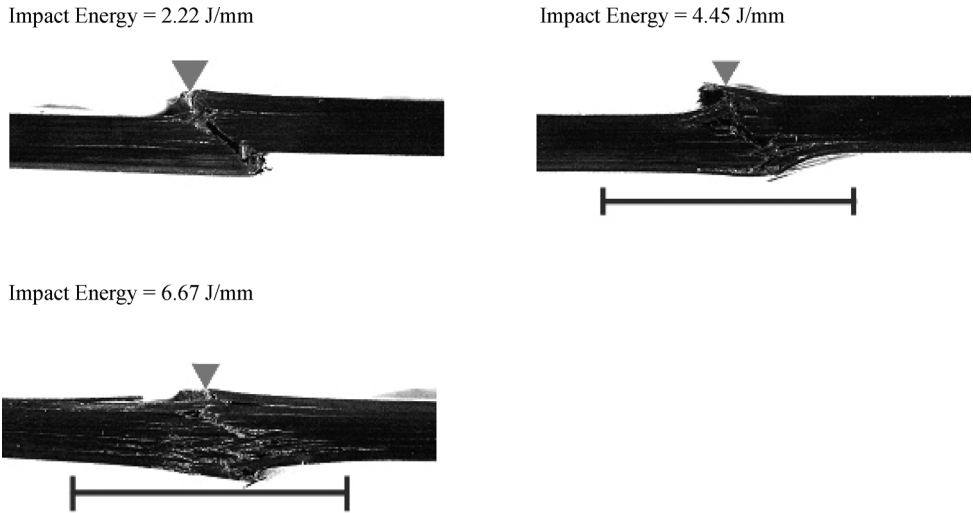


Figure 16. Impact damage and compressive failure observed on the cut section of the specimen after CAI tests at 180°C.

The C-scan inspection of the specimen impacted at 2.22 J/mm before the compression test found no delamination. In contrast, delamination was found in other specimens impacted at higher than or equal to 4.45 J/mm. However, the length of delamination was increased only a small amount by the compression test. All compressive failures macroscopically showed a shear failure mode regardless of the impact energy level and compression test temperature, though many small delaminations accompanied at the impact energy of 6.67 J/mm or higher. The swelling of failed specimens in the out-of-plane direction after compression tests

was rather small. Compression tests on CFRPs conducted by the authors at room temperature in the past [6, 7] have shown that large delaminations occurred and the specimen failed with out-of-plane buckling, and these had a rhombus shape as seen from the side. A failure mode like those in the present study was found only in the Hot/Wet compression tests of T800H/PMR-15 specimens [8].

The interesting compressive-failure behaviors described above are considered to be typical and fundamental for CFRPs using a highly tough resin, except under a Hot/Wet testing condition.

4. OVERALL DISCUSSION

Since PETI5 resin has high toughness, MR50K/PETI5 laminates should be highly resistant to shear stresses that are generated at the boundaries between the layers when an impact load is imposed. Let us discuss below how this characteristic appeared in the CAI behavior.

A possible reason why the compressive strength of a non-impacted MR50K/PETI5 coupon specimen is lower than that of a T800H/PMR-15 specimen is the difference in their failure modes. The compressive failure mode of the MR50K/PETI5 specimen macroscopically displayed shear fracture as shown in the side view. However, delamination buckling was the failure mode for the T800H/PMR-15 specimen [9] which occurred over a wide damage area. Inside of this damage area, a large amount of energy was accumulated up to the fracture point and released suddenly, and the damage area observed after fracture was very large. It is thought that the latter fracture mode allows the accumulation of a larger amount of energy inside the material prior to the fracture than the former fracture mode does.

Figures 4 and 5 show that the load response curves of the materials differ greatly. In the MR50K/PETI5 specimen, the load response curve shows a trapezoidal form against the time axis for the impact energy levels of 4.45–8.90 J/mm. The internal damage situation of MR50K/PETI5 laminates presented in Figs 8 and 9 after impact tests, and Figs 15 and 16 after CAI tests, indicates that it was mainly the deformation of PETI5 resin that absorbed much of the impact energy, because the delaminations generated by the shear fracture of the resin in the laminate were fairly small. Moreover, as mentioned before, much impact energy was absorbed by the resin damage as observed in the vicinity of the impacted surface.

On the other hand, T800H/PMR-15 in Fig. 5 displays a load response curve with a sinusoidal or triangular form with small saw-tooth waves superimposed. This load response curve and C-scan observation indicate that the impact energy was mainly absorbed by delamination, as shown in Fig. 9. Moreover, brittle resin failure accompanied transverse cracks in the layers. Several large delaminations occurred at layer boundaries, facilitating delamination buckling and resulting in the low CAI strength that was measured.

Figures 4, 8, 10, 11, 12, 13, 14, 15 and 16 revealed the following: Since the interlaminar fracture toughness of MR50K/PETI5 is very high, (1) the resin absorbs

much of the impact energy, (2) the delamination area produced by an impact load is small, (3) the delamination produced by the impact load progressed very little with in-plane compressive load, (4) final fracture was generated not by the delamination buckling but by macroscopic shear-type fracture, and (5) high CAI strength was observed. These are considered to be the typical features presented by composite materials using a highly tough resin.

The facts described above mean that if a highly tough resin like PETI5 is used for composite structures, the strength degradation resulting from the delamination generated by out-of-plane deformation, which is one of the weakest points of conventional CFRPs, can be greatly improved. That is, special strengthening measures for the laminate thickness direction, such as stitching, are not necessary in most composite structural designs.

5. CONCLUSIONS

This study experimentally investigated the CAI behavior of a MR50K/PETI5 carbon fiber/tough polyimide composite material. The CAI behaviors investigated include the impact load response, impact damage, CAI strength, and CAI fracture mode. The major results obtained are as follows:

- (1) When a MR50K/PETI5 specimen was impacted in the out-of-plane direction, visible damage appeared on the surface, though the delamination area was quite small. Observed with a 3D ultrasonic inspection system, the surface damage area was the same size as the delamination area inside of the specimen when impacted at 4.45 J/mm.
- (2) The delamination area of MR50K/PETI5 specimens impact-loaded at 4.45 J/mm was approximately 5% of that of T800H/PMR-15 specimens [4]. The large difference in the delamination area is considered to originate in the difference of resin toughness.
- (3) The impact-damage picture taken by the 3D ultrasonic inspection system clarified that the delamination progressed spirally clockwise from the top surface to the center and then counterclockwise from the center to the bottom surface. This was ascribed to the propagation of delamination occurring with a rotation from one layer to the next following small lamination angle differences originating in the stacking sequence.
- (4) The non-impacted compressive strength of MR50K/PETI5 at room temperature was lower by about 17% than that of T800H/PMR-15. The CAI strength of MR50K/PETI5 at room temperature when impact-loaded at 2.22–8.90 J/mm was approximately 1.6–2.2 times that of T800H/PMR-15, and the failure strain of MR50K/PETI5 was also higher. Thus, although the non-impacted compressive strength of MR50K/PETI5 was rather lower, the CAI strength and CAI failure strain were much higher than those of T800H/PMR-15. This is due to the high toughness of PETI5 resin, including the difference in failure modes.

- (5) The CAI strength and failure strain of MR50K/PETI5 at 180°C dropped to about 70–80% of those at room temperature. However, these values were far higher than those of the CAI strength and failure strain of T800H/PMR-15 even at room temperature.
- (6) The CAI strength of MR50K/PETI5 decreased linearly with increasing impact energy at room temperature and 180°C, even up to 8.90 J/mm at room temperature.
- (7) The compressive fracture mode of a non-impacted MR50K/PETI5 coupon specimen at room temperature is considered to be macroscopic shear fracture. On the other hand, examination of the cross-sectional area cut from the failure specimens after CAI tests clarified that the shear failure mode was macroscopically dominant regardless of the amount of impact energy and the test temperature. However, this failure was accompanied by additional delaminations, including a small amount of delamination when impact-loaded at an energy of 2.22 J/mm and numerous small delaminations when impact-loaded at 6.67 J/mm.
- (8) In MR50K/PETI5, the delamination length in the load-axis direction observed for the specimens after the impact and compression tests was only a small amount longer than just after the impact test.
- (9) Typical and fundamental CAI behaviors of a CFRP using PETI5, a highly tough resin, were clarified. This study demonstrated that if a highly tough resin is introduced into CFRP structures, the weak out-of-plane strength of CFRP structures can be greatly improved.

Acknowledgements

The authors greatly appreciate the kindness of Toshiba Corp., Industrial and Power Systems and Services Co., in taking 3D ultrasonic pictures of the damage state inside the impacted specimen.

REFERENCES

1. T. H. Hou, B. J. Jensen and P. M. Hergenrother, Processing and properties of IM7/PETI composite, *J. Compos. Mater.* **30**, 109–122 (1996).
2. S. P. Walker, Thermal effects on the compressive behavior of IM7/PETI laminates, in: *Proceedings of ICCM-14 No. 0859*, San Diego, CD-ROM (2003).
3. P. M. Hergenrother, Composites, adhesives, and sealants for high speed commercial airplanes, *Chemical Innovations* (Feb.), 34–44 (2000).
4. D. Kobayashi, Y. Hamaguchi and T. Shimokawa, CAI strength properties of a T800H/PMR-15 carbon/polyimide composite material at room and elevated temperatures, in: *Proceedings of 40th Aircraft Symposium*, JSASS/JAEA, pp. 565–568, CD-ROM (2002) (in Japanese).
5. N. Sugawara, T. Kamiyama, H. Nakajima, T. Matsushita, H. Mitsuma and T. Kobayashi, Mechanical properties and processing technologies of a high-temperature resin composite for

- HOPE structures, in: *Proceedings of 32nd JSASS/JSME Structures Conference*, Hiroshima, pp. 62–65 (1990) (in Japanese).
6. T. Shimokawa, H. Katoh, Y. Hamaguchi, S. Sanbongi, H. Mizuno, H. Nakamura and R. Asagumo, Effect of thermal cycling on microcracking and strength degradation of high-temperature polymer composite materials for use in next-generation SST structures, *J. Compos. Mater.* **36**, 885–895 (2002).
 7. C. Marais, T. Shimokawa and H. Katoh, Compressive strength/degradation relationship of carbon/BMI composites after thermal cycling and aging for the second generation SST structures, in: *Proceedings of ICCM-13*, ID1024, Beijing, CD-ROM (2001).
 8. T. Shimokawa, Y. Hamaguchi and H. Katoh, Effect of moisture absorption on hot/wet compressive strength of T800H/PMR-15 carbon/polyimide, *J. Compos. Mater.* **33**, 1685–1698 (1999).
 9. T. Shimokawa, Y. Hamaguchi and Y. Kakuta, Statistical evaluation of compressive mechanical properties of a T800H/PMR-15 carbon/polyimide composite, *J. Japan Soc. Compos. Mater.* **22**, 184–192 (1996) (in Japanese).